Nanotechnology

PAPER • OPEN ACCESS

Monitoring selective etching of self-assembled nanostructured a-Si:Al films

Recent citations

- Selective etching of nanostructured a-Si:Al and its effect on porosity, Al gradient and surface oxidation
T. Kjeldstad *et al*

To cite this article: T Kjeldstad *et al* 2019 *Nanotechnology* **30** 135601

View the article online for updates and enhancements.

IOP ebooks™

Bringing together innovative digital publishing with leading authors from the global scientific community.

Start exploring the collection–download the first chapter of every title for free.

This content was downloaded from IP address 37.191.140.97 on 18/05/2020 at 13:01

OPEN ACCESS
IOP Publishing

Nanotechnology

Nanotechnology 30 (2019) 135601 (5pp)

https://doi.org/10.1088/1361-6528/aafb86

Monitoring selective etching of self-assembled nanostructured a-Si:Al films

T Kjeldstad[1,3], A Thøgersen[2], M Stange[2], A Azarov[1], E Monakhov[1] and A Galeckas[1]

[1] Department of Physics/Centre for Materials Science and Nanotechnology, University of Oslo, PO Box 1048 Blindern, NO-0316 Oslo, Norway
[2] SINTEF Materials and Chemistry, PO Box 124 Blindern, NO-0314 Oslo, Norway

E-mail: torunn.kjeldstad@smn.uio.no

Received 28 August 2018, revised 10 December 2018
Accepted for publication 2 January 2019
Published 1 February 2019

Abstract

Nanoporous and nanowire structures based on silicon (Si) have a well recognized potential in a number of applications such as photovoltaics, energy storage and thermoelectricity. The immiscibility of Si and aluminum (Al) may be utilized to produce a thin film of vertically aligned Al nanowires of 5 nm diameter within an amorphous silicon matrix (a-Si), providing a cheap and scalable fabrication method for sub 5 nm size Si nanostructures. In this work we study functionalization of these structures by removal of the Al nanowires. The nanowires have been etched by an aqueous solution of HCl, which results in a structure of vertically aligned nanochannels in a-Si with admixture of SiO_x. The removal of Al nanowires has been monitored by several electron microscopy techniques, x-ray diffraction, Rutherford backscattering spectroscopy, and optical reflectance. We have established that optical reflectance measurements can reliably identify the complete removal of Al, confirmed by other techniques. This provides a robust and relatively simple method for controlling the nano-fabrication process on a macroscopic scale.

Keywords: amorphous Si, aluminum, nanowires, porous silicon, solar cells, self-organization

(Some figures may appear in colour only in the online journal)

Introduction

The optical properties of silicon (Si) nanostructures are widely researched towards utilizing silicon in photonics and optimizing absorption properties in thin film silicon solar cells [1]. Specifically, reducing the dimensions of Si to the quantum confinement regime in order to increase and change the bandgap type from indirect to direct is particularly interesting for such applications [2–4]. Si nanostructures have also been suggested incorporated into e.g. energy storage devices and thermoelectric materials [5–8].

[3] Author to whom any correspondence should be addressed.

Original content from this work may be used under the terms of the Creative Commons Attribution 3.0 licence. Any further distribution of this work must maintain attribution to the author(s) and the title of the work, journal citation and DOI.

Various fabrication methods have been developed to achieve '<5 nm size' silicon structures such as porous Si [9–11], Si nanowalls [3], nanowires [12] and quantum dots [4]. Self-assembly approach has already shown a great potential for fabrication of a broad range of nanostructured films and composite materials: from organic–inorganic structures [13–15] to pure inorganic based systems [16, 17]. Nanoporous amorphous Si (a-Si) consisting of parallel vertically aligned channels may be fabricated via nanophase separation between aluminum (Al) and Si and subsequent selective etching of Al [18]. The structure arises from self-assembly of Al nanowires which are formed in the a-Si due to the low solubility of Si and Al in the solid state [19]. The Al wires grow perpendicularly to the substrate surface and stretch over the film thickness. Previous reports have demonstrated the fabrication of such structures by magnetron sputtering and filtered cathodic vacuum arc deposition [18, 20]. Thøgeresen *et al* have recently demonstrated that Al

 © 2019 IOP Publishing Ltd Printed in the UK

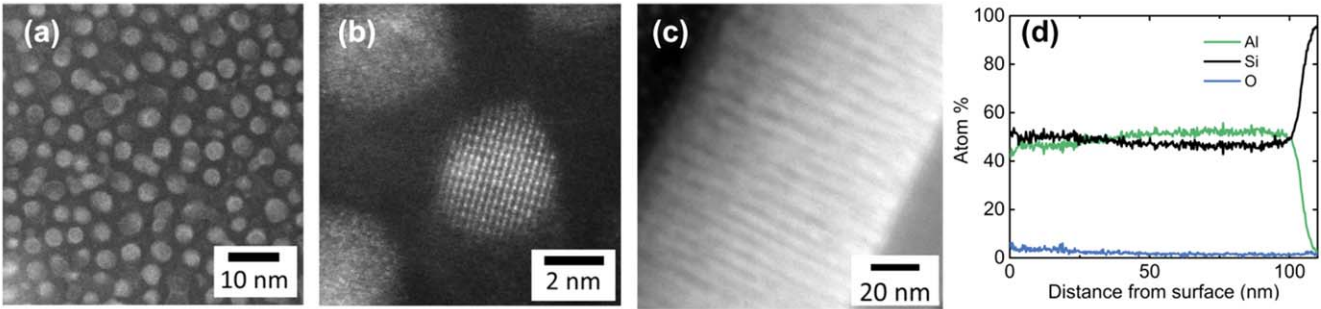

Figure 1. Top view HRTEM (a) and (b) and cross-section HAADF STEM (c) images and EDS stoichiometry profile (d) for the as-grown aSi:Al film.

nanowires with 5 nm diameter within an a-Si framework may be fabricated by co-sputtering of Al and Si at room temperature [21].

In this study we investigate functionalization of the a-Si nanostructure by removing Al with wet chemical etching. We have fabricated nanoporous films with well-aligned, evenly distributed, straight pores with a diameter of ~5 nm and a length of 100 nm. The structures have been characterized by transmission electron microscopy (TEM), Rutherford backscattering spectrometry (RBS), x-ray diffraction (XRD) and ultraviolet-visible-near infrared spectrophotometry (UV–vis-NIR). We demonstrate that the removal of Al-nanowires can be monitored by relatively simple optical measurements, thus providing a robust and simple method for controlling the nano-fabrication process on a macroscopic scale.

Methods

Si and Al were co-sputtered by a CVC 601 magnetron sputtering system onto single crystalline p-Si (100) substrates. The system consisted of two 8″ targets with normal sputter angle and 6 cm distance between substrate and targets. The deposition was performed at room temperature with thin alternating layers with a ratio of approximately 40 atomic % Al and 60 atomic % Si obtained by a power of 400 W for Si and 150 W for Al with a substrate rotation of 2.5 rpm and a sputtering time of 22 min. The rotation speed corresponds to deposition of Al and Si layers of about 1 nm, but segregation between the elements is observed as particle formation rather than layer formation. For a more detailed description of the deposition process see [12]. The sputtering process was carried out in an argon atmosphere at 3 mTorr and with a hydrogen flow of 4 ml min^{-1}. Formation of Al nanowires was confirmed by TEM. Al was removed by a wet etch process in a 1:1 solution of 37% HCl in deionized water. Changes in etching conditions during etching is considered to be negligible (Al content $<1{:}10^6$). The etching process was done at room temperature without agitation of the solution. After etching, the samples were rinsed in deionized water.

High resolution TEM (HRTEM), high angled annular dark field (HAADF) scanning TEM (STEM), and energy dispersive spectroscopy (EDS) was performed using a FEI Titan G2 60-300 microscope with a super EDS detector. The cross-sectional samples were prepared by grinding and ion-milling using a Gatan precision ion position system with 4 kV gun voltage.

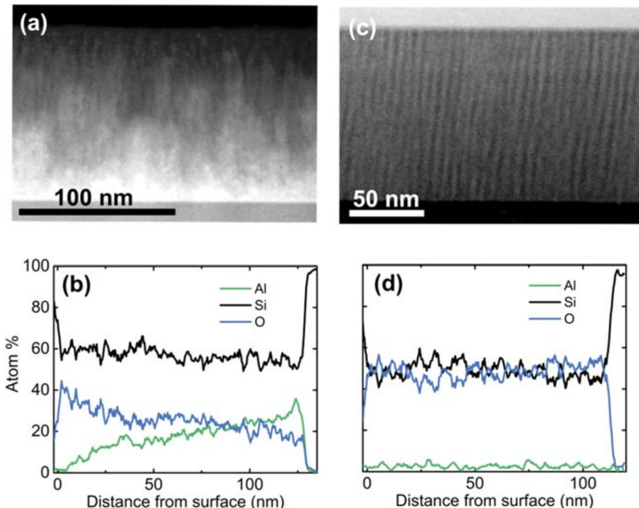

Figure 2. Cross-sectional HAADF STEM image (a) and a corresponding EDS line scan (b) of a-Si:Al film etched for 4 h. Cross-sectional TEM image (c) and a corresponding EDS line scan (d) for a a-Si:Al film etched for 30 h.

Optical characterization was performed by measuring total reflectance at room temperature using a Shimadzu SolidSpec-3700/3700DUV spectrophotometer with a wavelength range of 186–2500 nm and fitted with an integral sphere.

XRD with a Rigaku MiniFlex 600 (Cu Kα-radiation, $\lambda = 1.54$ Å) was used to analyze Al nanowires. The samples stoichiometry was analyzed by RBS with 1.62 MeV $4He^+$ ions backscattered into a detector positioned at 165° relative to the incident beam direction. Composition of the films was determined from the experimental spectra using simulations performed with the SIMNRA code [22] without taking into account a porosity of the films.

Results and discussion

Figure 1 shows TEM results for an as-grown sample. In the HAADF STEM cross-sectional images of the as-deposited

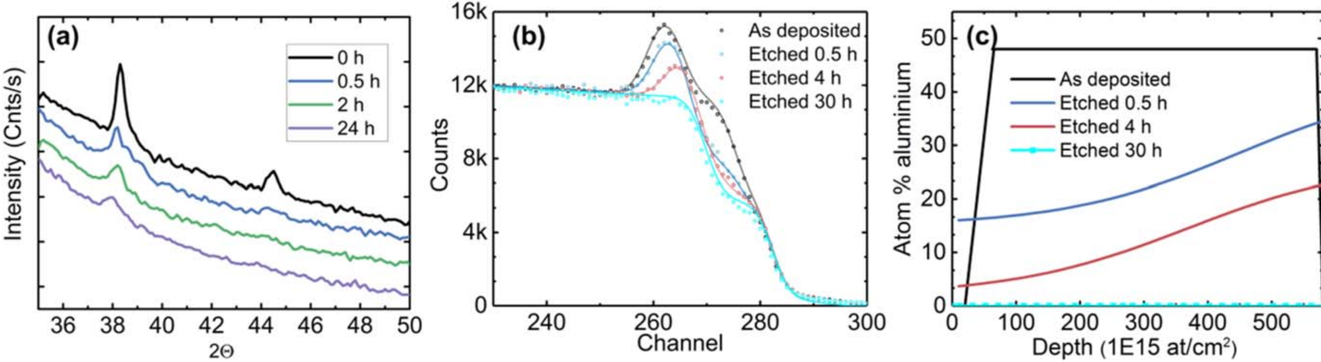

Figure 3. (a) XRD, (b) RBS and (c) Al depth distributions used for fitting the measured RBS spectra, of samples etched in HCl for 0–30 h.

a-Si:Al film (figure 1(c)) one can observe Al-nanowires as bright threads that cross through the 100 nm film. The top view image in figure 1(a) shows that the wires are evenly distributed in the film and that the diameter of the nanowires is around 5 nm. The HRTEM image in figure 1(b) indicates that the Al-nanowires are crystalline. The crystallinity of the wires is further demonstrated and discussed in [12]. EDS measurements (figure 1(d)) confirm a close to uniform distribution of Al over the film thickness, as well as the 50:50 ratio between Si and Al in the film stoichiometry. These observations are consistent with those reported previously [18, 20] and demonstrate reproducibility and robustness of the growth method.

Treatment of the sample in the HCl solution results in etching of the Al nanowires (figure 2). Figure 2(a) shows a HAADF STEM cross-sectional image of a sample etched in HCl for 4 h. The brighter contrast areas indicate the presence of Al. The image shows that the performed etching results in partial removal of Al, leaving residual Al in the nanochannels deeper in the film. It can also be observed that the etching process does not seem to remove the Al uniformly in different nanochannels. The EDS line scan presented in figure 2(b) shows that the overall Al-concentration increases gradually towards the substrate. In addition, the oxygen concentration inversely follows the Al concentration, indicating oxidation of the exposed a-Si. If etched for a sufficient period of time, the Al in the nanochannels may be removed as shown in the cross-sectional TEM image of a sample etched for 30 h (figure 2(c)). This observation is supported by the EDS line scan in figure 2(d), which shows that Al is removed, and the EDS signal is below the detection limit. The required etching time is determined by the rate of transport of etchant in the nanochannels, and due to the narrow channel width, the etching rate is slower than the common etching rate of Al [23, 24]. The EDS line scan also shows a homogenous level of O and Si throughout the film and corresponding x-ray photoelectron spectroscopy (not shown here) shows that the film consists of both SiO_x and a-Si. Thus, complete etching results in a homogenous film with unfilled straight nanochannels in the a-Si framework.

The results from electron microscopy measurements are complemented and supported by other techniques (figure 3). From XRD measurements presented in figure 3(a) it is clear that the intensity of the Al reflections (111) and (200) is reduced with increasing etching time, indicating a gradual reduction in Al content. RBS was used to analyze the depth distribution of Al through the film. Figure 3(b) shows RBS spectra for the as-deposited sample and samples etched for 0.5, 4 and 30 h. The Al concentration profiles deduced from the fitting of the RBS measurements are shown in figure 3(c). The Al profile after 4 h is consistent with the EDS line scan showed in figure 2(c). After 30 h of etching, there is no measured response from Al in the sample.

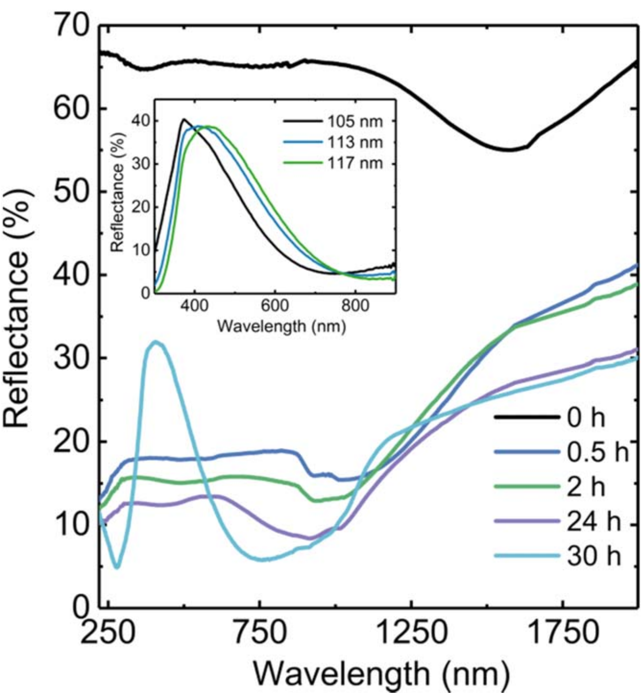

Figure 4. Reflectance as a function of etching time. Insert shows reflectance of samples with Al removed of thickness 105–117 nm. Thickness was measured by x-ray reflectivity prior to Al removal.

Wet chemical etching has a significant effect on the optical properties of the structures, in particular on the reflectance (figure 4). The as-grown aSi:Al films exhibit a reflectance of around 60%–65% within a wide spectral range. However, already a short etching time (0.5 h) results in a considerable decrease of the reflectance down to 15%–20% in

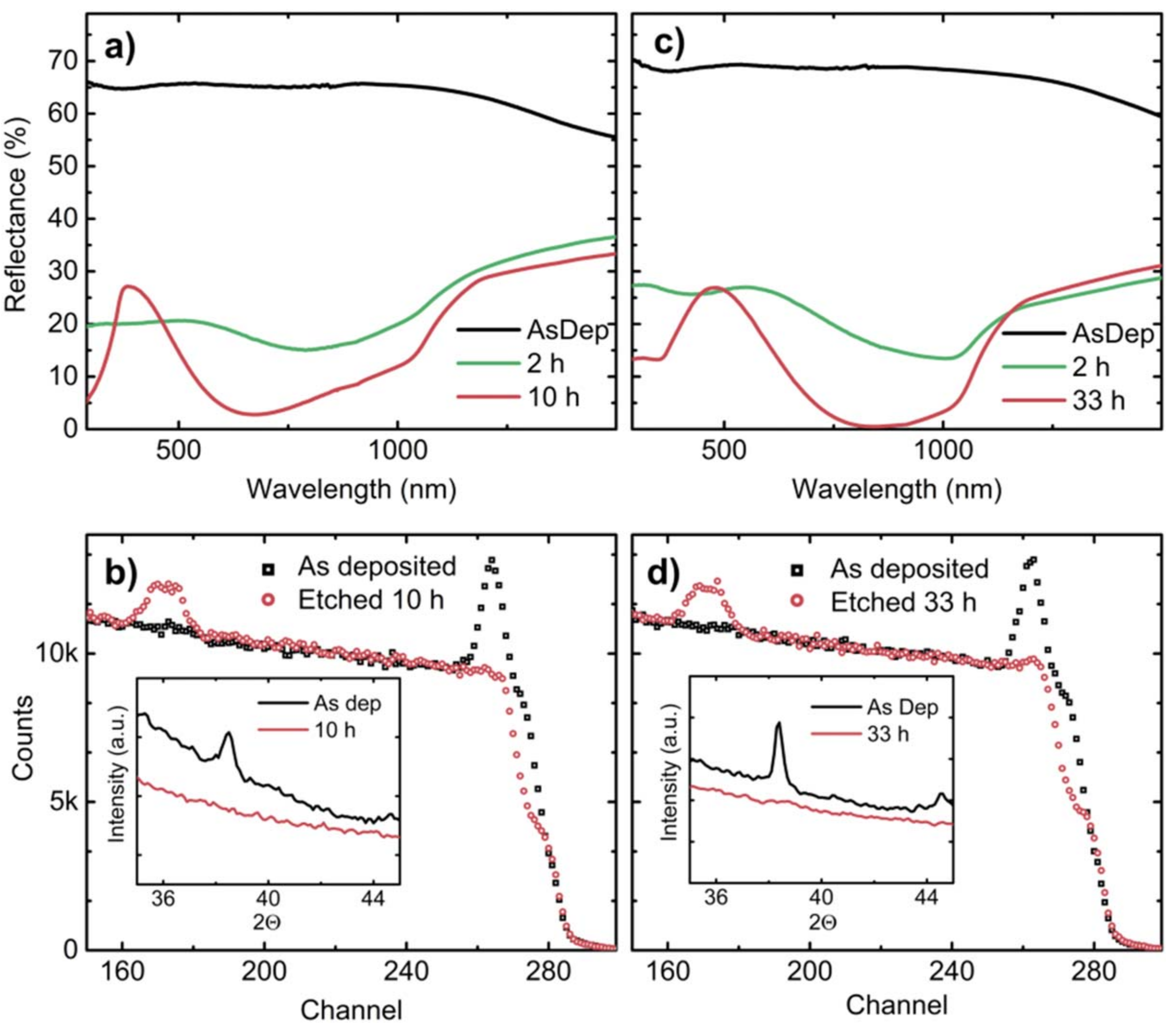

Figure 5. Reflectance (a), (c) and RBS (b), (c) of sample set 2 and 3 etched in HCl for 0–10 h and 0–33 h. Inset shows XRD before and after Al removal.

the spectral range from UV to NIR (200–1000 nm) and gradually decreases further with increase of the etching time. Clearly, the reduction of reflectance is in direct relation with the reduction of Al content in the nanochannels according to TEM, XRD and RBS measurements. The likely cause of this effect is a gradient in refractive index due to varying Al and oxide (Al_2O_3 and SiO_x) content introduced by the etching [25]. In addition, plasmonic scattering and absorption at the Al nanowires in the a-Si matrix may contribute to the observed decrease in reflectance [26, 27]. After etching for 30 h, however, we observe a dramatic change in the reflectance. It shows a strong dependence on the wavelength, consistent with and governed by the interference. This is supported by an observed shift in reflectance peak with increased thickness (shown in inset in figure 4). The change in the reflectance coincides with the removal of Al nanowires observed by TEM and EDS (figures 2(c), (d)). Measurements of diffuse reflectance have not revealed any significant change for as-deposited, partly, and fully etched samples.

The correlation between optical properties and Al content is confirmed for several other samples (figure 5). Figure 5(a) confirm the decrease in reflectance in the UV and visible range after a short etching time, until the appearance changes towards a strong wavelength dependent peak for two different sample sets. The removal of Al at this point is supported by RBS and XRD measurements which are shown in figures 5(b) and (d). It can be noted that the etching time needed for complete Al removal differs between the sample sets. Preliminary investigations suggest that the difference in required etching time is due to minor difference in the microstructure of the nanowires [28]. Nevertheless, the optical reflectance measurements have reliably identified the removal of Al from the nanowires.

Conclusion

In conclusion, we have studied functionalization of self-assembled nanostructured a-Si:Al films. The Al nanowires, formed in the course of magnetron sputtering of a-Si:Al films have been etched by an aqueous solution of HCl resulting in a structure of vertically aligned nanochannels. The removal of

Al from the nanowires has been monitored by several techniques. It has been established that optical reflectance measurements can reliably identify the removal of Al, thus providing a relatively simple method of controlling the fabrication process on a macroscopic scale.

Acknowledgments

This work was funded by the Research Council of Norway through the funding program FRINATEK, project No. 231658. The Research Council of Norway is also acknowledged for the support to the Norwegian Micro- and Nano-Fabrication Facility, NorFab, project No. 245963.

ORCID iDs

T Kjeldstad https://orcid.org/0000-0002-3716-5322
A Thøgersen https://orcid.org/0000-0002-4064-1887

References

[1] Priolo F, Gregorkiewicz T, Galli M and Krauss T F 2014 Photonics and photovoltaics *Nat. Nanotechnol.* **9** 19–32
[2] Bisi O, Ossicini S and Pavesi L 2000 Porous silicon: a quantum sponge structure for silicon based optoelectronics *Surf. Sci. Rep.* **38** 1–126
[3] Kanematsu D, Yoshiba S, Hirai M, Terakawa A, Tanaka M, Ichikawa Y, Miyajima S and Konagai M 2016 Observation of quantum size effect from silicon nanowall *Nanoscale Res. Lett.* **11** 530
[4] Barbagiovanni E G, Lockwood D J, Simpson P J and Goncharova L V 2014 Quantum confinement in Si and Ge nanostructures: theory and experiment *Appl. Phys. Rev.* **1** 11302
[5] Au M, McWhorter S, Ajo H, Adams T, Zhao Y and Gibbs J 2010 Free standing aluminum nanostructures as anodes for Li-ion rechargeable batteries *J. Power Sources* **195** 3333–7
[6] Banerjee P, Perez I, Henn-Lecordier L, Lee S B and Rubloff G W 2009 Nanotubular metal–insulator–metal capacitor arrays for energy storage *Nat. Nanotechnol.* **4** 292
[7] Boukai A I, Bunimovich Y, Tahir-kheli J, Yu J, Goddard W A III and Heath J R 2008 Silicon nanowires as efficient thermoelectric materials *Nature* **451** 168–71
[8] Ge M, Rong J, Fang X and Zhou C 2012 Porous doped silicon nanowires for lithium ion battery anode with long cycle life *Nano Lett.* **12** 2318–23
[9] Cullis A G, Canham L T and Calcott P D J 1997 The structural and luminescence properties of porous silicon *J. Appl. Phys.* **82** 909–65
[10] Wehrspohn R B, Chazalviel J N, Ozanam F and Solomon I 1996 Conditions of elaboration of luminescent porous silicon from hydrogenated amorphous silicon *Phys. Rev. Lett.* **77** 1885–8
[11] Kanemitsu Y 1995 Light emission from porous silicon and related materials *Phys. Rep.* **263** 1
[12] Ma D D D, Lee C S, Au F C K, Tong S Y and Lee S T 2003 Small-diameter silicon nanowire surfaces *Science* **299** 1874–7
[13] Chen K, Li J, Zhang L, Xing R, Jiao T, Gao F and Peng Q 2018 Facile synthesis of self-assembled carbon nanotubes/dye composite films for sensitive electrochemical determination of Cd (II) ions *Nanotechnology* **29** 445603
[14] Luo X, Ma K, Jiao T, Xing R, Zhang L, Zhou J and Li B 2017 Graphene oxide-polymer composite langmuir films constructed by interfacial thiol-ene photopolymerization *Nanoscale Res. Lett.* **12** 99
[15] Zhou J, Gao F, Jiao T, Xing R, Zhang L and Zhang Q 2018 Selective Cu (II) ion removal from wastewater via surface charged self-assembled polystyrene-Schiff base nanocomposites *Colloids Surf.* A **545** 60–7
[16] Fukutani K, Ishida Y, Tanji K and Den T 2007 Nanowire array fabricated by Al–Ge phase separation *Thin Solid Films* **515** 4629–35
[17] Tian Y, Mukherjee P, Jayaraman T V, Xu Z, Yu Y, Tan L, Sellmyer D J and Shield J E 2014 Ultrahigh-density sub-10 nm nanowire array formation via surface- controlled phase separation *Nano Lett.* **14** 4328–33
[18] Fukutani K, Tanji K, Motoi T and Den T 2004 Ultrahigh pore density nanoporous films produced by the phase separation of eutectic Al–Si for template-assisted growth of nanowire arrays *Adv. Mater.* **16** 1456–60
[19] Murray J L and McAlister A J 1984 The Al–Si (aluminum–silicon) system *Bull. Alloy Phase Diagr.* **5** 74
[20] Saito T, Horie R, Den T, Bendavid A, Preston E and Martin P J 2009 Phase separated AlSi thin films prepared by filtered cathodic arc deposition *Thin Solid Films* **517** 1567–71
[21] Thøgersen A, Jensen I J T, Stange M, Kjeldstad T, Martinez-Martinez D, Løvvik O M, Ulyashin A G and Diplas S 2018 Formation of nanoporous Si upon self-organized growth of Al and Si nanostructures *Nanotechnology* **29** 315602
[22] Mayer M 2019 SIMNRA version 6.06
[23] Walker P and Tarn W H 1991 *Handbook of Metal Editors* (Boca Raton, FL: CRC Press)
[24] Westberg D, Paul O, Andersson G I and Baltes H 1996 Surface micromachining by sacrificial aluminium etching *J. Micromech. Microeng.* **6** 376–84
[25] Raut H K, Ganesh V A, Nair A S and Ramakrishna S 2011 Anti-reflective coatings: a critical, in-depth review *Energy Environ. Sci.* **4** 3779
[26] Villesen T F, Uhrenfeldt C, Johansen B and Nylandsted Larsen A 2013 Self-assembled Al nanoparticles on Si and fused silica, and their application for Si solar cells *Nanotechnology* **24** 1–5
[27] Van Der Vliet T and Vece M D 2016 Shifting the aluminum nanoparticle plasmon resonance to the visible with SiN and a-Si thin films *Thin Solid Films* **603** 404–7
[28] Fukutani K, Tanji K, Saito T and Den T 2008 Fabrication of well-aligned Al nanowire array embedded in Si matrix using limited spinodal decompositon *Japan. J. Appl. Phys.* **47** 1140–6